Plasma spectroscopy in the conditions of the ITER tokamak

2012 J. Phys.: Conf. Ser. 399 012019

(http://iopscience.iop.org/1742-6596/399/1/012019)

Plasma spectroscopy in the conditions of the ITER tokamak

J Rosato[1], Y Marandet[1], V Kotov[2], D Reiter[2], H Capes[1], L Godbert-Mouret[1], M Koubiti[1], R. Hammami[1] and R Stamm[1]

[1]Laboratoire PIIM, UMR 7345 Université d'Aix-Marseille / CNRS, Centre de Saint-Jérôme, Case 232, F-13397 Marseille Cedex 20, France

[2]IEK-4, Forschungszentrum Jülich GmbH, Trilateral Euregio Cluster, Euratom Association, D-52425 Jülich, Germany

E-mail: joel.rosato@univ-amu.fr

Abstract. The state of art of the line shape modeling techniques involved in tokamak edge plasma spectroscopy is reported, in the context of the preparation for ITER. Hydrogen spectra are calculated assuming a line-of-sight crossing a 2D-plasma background obtained from numerical simulations. The Doppler, Zeeman and Stark effects are retained. The possibility for a line shape-based diagnostic of the ITER divertor plasma is examined through fittings of simulated spectra and comparison with the input plasma fields. The role of turbulent fluctuations on line shapes is also examined.

1. Introduction

ITER is an international project aimed at demonstrating the principle of producing more energy from the fusion process than is used to initiate it. The tokamak, presently under construction in Cadarache (France), will be equipped with an extensive set of plasma diagnostics [1]. Passive spectroscopy of the hydrogen Balmer lines with a low upper principal quantum number n (in particular, the Hα transition) is presently considered to measure fluxes of the hydrogen isotopes and to determine the isotopic proportion of the fuelling gas (N_T/N_D,N_H/N_D) in the divertor region. Furthermore, information on the electron density N_e will be available through the analysis of the Stark broadening of high-n lines. Such lines are already observed in present divertor plasmas in the so-called "detached regime", e.g. in JET [2] and Alcator C-Mod [3]. A well-known difficulty that occurs in the interpretation of an observed spectrum is provided by the non-uniformity of the plasma along the line-of-sight. Recently, this issue has been investigated numerically for plasma conditions relevant to ITER, by using a line shape code and the transport code B2-EIRENE [4]. The possibility for a line shape-based diagnostic has been demonstrated, at least in one typical plasma background [5,6]. An additional difficulty in the interpretation of spectra is provided by the presence of turbulent fluctuations. Efforts have been undertaken in recent years in order to retain low-frequency fluctuations on line shapes [7–9]. In this work, we report on the modeling techniques involved in tokamak edge plasma spectroscopy with a special emphasis on hydrogen lines. Section 2 gives an overview on the physical mechanisms leading to line broadening. Next, we simulate spectra resulting from a line-of-sight crossing the ITER divertor (Sec. 3) and we examine the possibility for a diagnostic by performing fittings of the simulated spectra to recover plasma parameters from the line shape (Sec. 4). An investigation of the role of turbulent fluctuations on spectral lines is presented in Sec. 5.

2. Line broadening mechanisms

The line broadening mechanisms are due to the physical processes that affect the emitting atomic species at the microscopic scale. These processes include the perturbation of the energy levels induced by the plasma's microscopic electric field (Stark effect) and the magnetic field (Zeeman effect), and the thermal motion of the emitters (Doppler effect). The common description of spectral line shapes relies on a quantum statistical formalism [10]. In the atom's frame of reference, a line shape can be written as the Fourier transform of the dipole autocorrelation function

$$I_0(\omega) = \frac{1}{\pi}\mathrm{Re}\int_0^\infty dt \mathrm{Tr}\left\{\rho\vec{d}_\perp \cdot U^+(t)\vec{d}_\perp U(t)\right\}e^{i\omega t}. \quad (1)$$

Here, ρ is the atomic density operator, $\vec{d}_\perp$ is the dipole projected onto the plane perpendicular to the radiation's propagation direction, the trace is performed over the atomic states of the upper level of the transition, the brackets {...} denote a classical average over the perturber trajectories (semi-classical approximation), and $U(t)$ is the evolution operator. It obeys the time-dependent Schrödinger equation

$$i\hbar\frac{dU}{dt}(t) = (H_0 + V(t))U(t), \quad (2)$$

where $H_0 = H_{\mathrm{at}} - \vec{\mu}\cdot\vec{B}$ is the Hamiltonian including both the atomic energy level structure and the Zeeman effect, and $V(t) = -\vec{d}\cdot\vec{E}(t)$ is the time-dependent Stark effect term resulting from the action of the microscopic electric field $\vec{E}(t)$. The line shape is the laboratory frame (i.e., accounting for the Doppler effect) is obtained by convolution with the atoms' velocity distribution function $f(\vec{v})$:

$$I(\omega) = \int d^3v f(\vec{v}) I_0(\omega - \omega_0 \vec{v}\cdot\vec{n}/c). \quad (3)$$

Here, ω_0 stands for the central frequency and $\vec{n}$ is a unitary vector along the propagation direction.

In tokamak edge plasmas, the typical densities and temperatures are such that the contribution of the electrons to Stark broadening can generally be described with an impact collision operator. Namely, for most of the observed Balmer lines, one has $\rho_{We} << r_0$ and $\tau_{ce} << \tau_i$ where ρ_{We}, r_0, τ_{ce} and τ_i are respectively the electron Weisskopf radius, the mean interparticle distance, the electron collision time and the time of interest at half-maximum (of the Doppler-free profile I_0). This amounts to performing the substitution $V(t) \to -iK_e - \vec{d}\cdot\vec{E}_i(t)$ where $\vec{E}_i(t)$ is the microfield due to the ions only and K_e is a constant operator denoting the electronic contribution, described as a series of short-time binary interactions. The impact approximation ceases to be valid only for very high-n lines, which will not be considered hereafter.

The ion contribution to Stark broadening is strongly dependent on the upper principal quantum number of the line under consideration. The Stark broadening is generally affected by the ion dynamics, which leads to a much broader and less structured line shape than expected from the quasi-static theory (which assumes $\vec{E}_i(t) \approx \vec{E}_i(0)$). The latter is only valid for high-n lines (typically $n >$ 10). In the following, we shall retain the ion dynamics on the low-n lines by using the simulation method, which consists of solving the time-dependent Schrödinger equation numerically with an electric field obtained from particle simulation [11–13]. The code used here has been designed essentially for weakly-coupled magnetized hydrogen plasmas and can be applied to tokamak divertor conditions [14]. The ions are described with a quasi-particle model, and the electron contribution is retained in the Schrödinger equation with the Griem-Kolb-Shen collision operator model [15].

In ITER, a correct estimation of the Stark effect will be critical, because the latter at high density can be of the same order as the Doppler broadening (which is traditionally assumed to be dominant in the case of low-n Balmer lines). This point is illustrated in Fig. 1. The Dα line profile obtained using various degrees of accuracy in the line broadening description is plotted at $N_e = 3.5\times10^{15}$ cm^{-3}, $T_e = T_i = T_{\mathrm{at}} = 1$ eV, B = 8 T and in perpendicular observation. The line has a Lorentz triplet structure due to the magnetic field which, as shown in the figure, for each component has a width at half maximum

about two times larger when the Stark effect is retained. For higher principal quantum number, the Stark broadening becomes more important and tends to dominate the Zeeman splitting (Fig. 2).

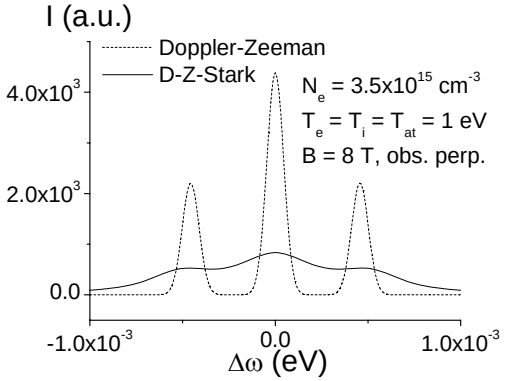

Figure 1. The contribution of the Stark effect to the line broadening is important on Dα and generally dominant on the other lines of the Balmer series. Here, plot of Dα using different degrees of accuracy on the line shape description.

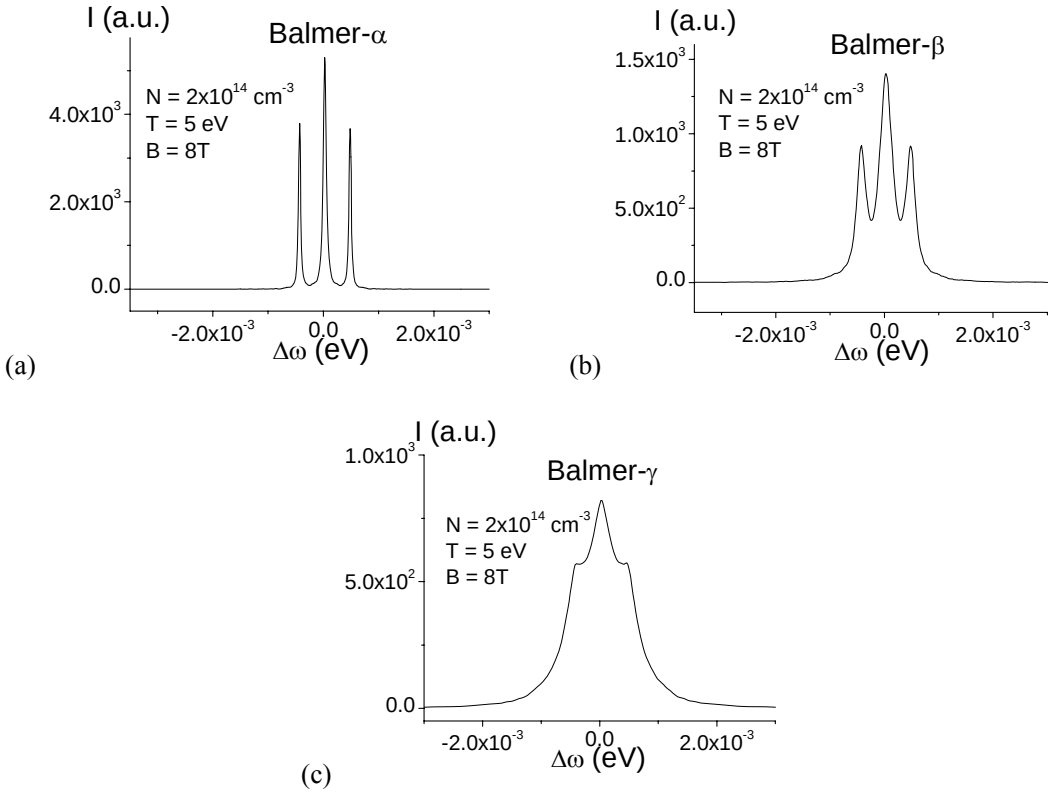

Figure 2. Plot of line shapes with increasing upper principal quantum number: (a) Balmer-α (n = 3), (b) Balmer-β (n = 4), (c) Balmer-γ (n = 5), in the atom's frame of reference, i.e. without Doppler effect. The Stark broadening increases with the principal quantum number and tends to dominate the Zeeman effect.

3. Simulation of an observed spectrum

In order to investigate the role of plasma non-uniformity along the line-of-sight, we have to consider a plasma background relevant to the divertor region and we have to perform a spatial integration. We have done so by using the transport code B2-EIRENE, which is extensively used for design relevant modeling of the ITER edge and divertor plasma [4]. Basically, it is a package formed by a Monte-Carlo solver for kinetic transport (EIRENE) and a two-dimensional plasma fluid code (B2). The EIRENE part solves a linear kinetic Boltzmann equation for the neutrals (atoms, molecules and also photons of the Lyman series) assuming a given plasma background and constructs, by Monte-Carlo method, quantities of interest like spatial distributions of reaction rates and energy and momentum sinks or sources. The presence of various energy levels is retained through the use of an equilibrium collisional-radiative model, accounting for both atoms and molecules. The obtained quantities of interest (e.g. particle sources for charged species) are then used in B2 as source and loss terms so that the fluid equations for charged particles can be solved. Obviously, the system formed by the neutral gas and the plasma is nonlinear, so that the solution is obtained by iterations. In general, the result of B2-EIRENE simulations leads to divertor plasma in recombining regime close to the target plates (see Fig. 3), with a high electron density (up to 3×10^{15} cm^{-3}) and a low temperature (down to 1 eV and smaller). The corresponding atomic density (hence, the emissivity) is concentrated in this zone. The dotted line in Fig. 3 denotes the line-of-sight considered in the present work.

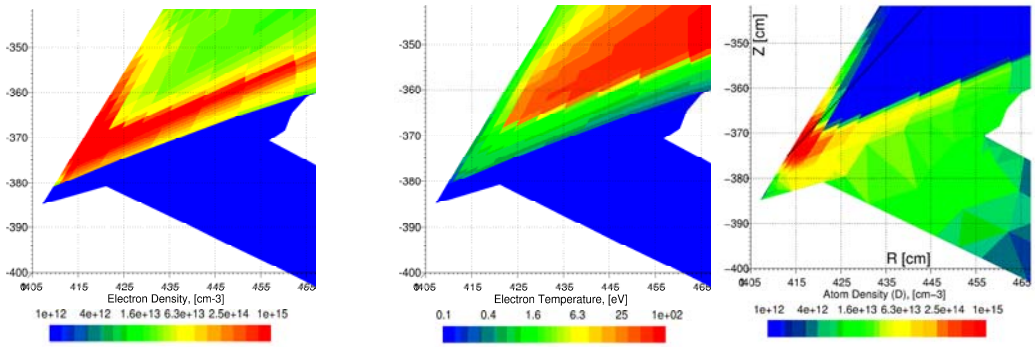

(a) (b) (c)

Figure 3. The B2-EIRENE calculations lead to a plasma in recombining regime, i.e. with a high density and a low temperature, close to the divertor target plates. Here, the spatial profile of the electron density (a) and temperature (b) and the atomic density (c) obtained from the calculation reported in [4] are shown. The zone corresponds to the vicinity of the inner target plate. The dotted line denotes the line-of-sight considered in this work.

4. Fitting of simulated spectra

Based on these transport simulations, we have calculated Dα assuming a passive observation on the line-of-sight shown in Fig. 3. The interesting property of passive spectroscopy is that it provides information on the plasma without perturbing it, provided that a suitable line shape model is employed. Here we present an analysis of Dα using a three-Voigt function model, accounting for Zeeman, Doppler and Stark effects. This model contains four independent parameters, namely the separation between the three components, the Gaussian width, the Lorentzian width and the relative amplitude of the lateral components. We have used a genetic algorithm routine [16]. The obtained result (Fig. 4) indicates that the fitted spectrum is in a quite good agreement with the "observed" spectrum from our modeling. The inferred atomic temperature extracted from the Gaussian width is about 1 eV, which correlates well with the temperature at the densest location on the line-of-sight, i.e. within about 10%. The magnetic field and angle of observation $\theta = (\vec{B}, \vec{n})$ extracted from the fitting analysis are 8.4 T and 77°, respectively, which also roughly corresponds to the correct local value at the emission zone, within 10%. As concerning the Lorentzian width, it should be noticed that its

interpretation using a Stark model is not obvious, since, as mentioned above, an analytical model cannot be used in general. The use of the impact approximation leads to underestimating the density by one order of magnitude, whereas, on the other hand, the quasi-static approximation provides the correct order of magnitude, but with a discrepancy still of about 50%. The situation is quite different for the lines with a high upper principal quantum number observed in detached regime, whose Stark analysis provides the density with a good accuracy. For example, an analysis of a simulated profile of D_{10} (deuterium Balmer 10 line, $n = 10 \rightarrow 2$ transition) done with the semi-empirical formula $\Delta\omega_{1/2} = C_1 N_e + C_2 N_e^{2/3}$ (here: $\Delta\omega_{1/2}$ is the half-width at half-maximum, the C_1 and C_2 constants which correspond to the electrons' and the ions' contribution to the Stark broadening, respectively) has provided a density of 3.4×10^{15} cm^{-3}, which correlates well with the densest location on the line-of-sight (Fig. 5).

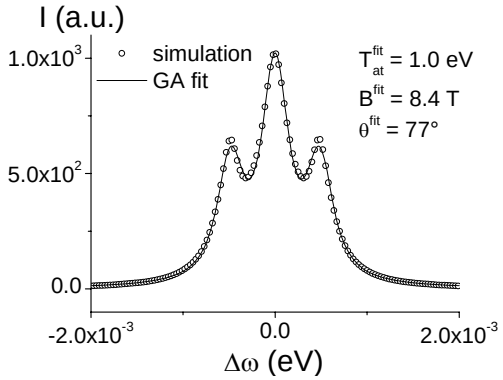

Figure 4. Fitting of the simulated observation (circles) by a three-Voigt function model (line). The fitted model-spectrum is in a good agreement with the simulated one, and the obtained plasma parameters T_{at}^{fit}, B^{fit}, θ^{fit} correspond closely to their value at the densest location on the line-of-sight.

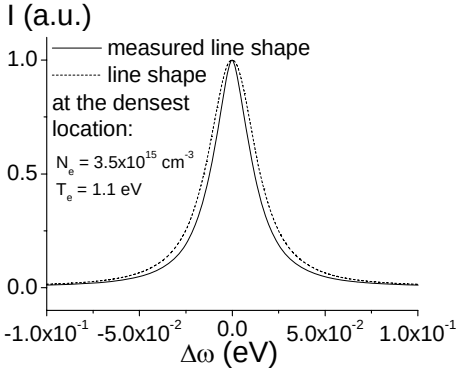

Figure 5. Plot of the D_{10} line shape. Here the measured line shape, i.e. resulting from integration along the line of sight, is close to that at the densest location.

5. Line shapes and turbulence

A major issue in magnetic fusion concerns the control of the instabilities induced by plasma edge turbulence. Recent works have been devoted to the description of passive spectroscopy signals in the presence of low-frequency fluctuations [7–9], aiming at providing a non-intrusive diagnostic

capability or for tests of the spectroscopy models neglecting turbulence. The formalism developed in these investigations relies on a statistical modeling of the fluctuations along the line-of-sight. A measured line shape is described with the following integral:

$$I_{\mathrm{mes}}(\omega) = \int dX W(X) B(X) I(\omega, X) . \qquad (4)$$

Here $X = (N_e, T_e \ldots)$ stands for the fluctuating parameters, $W(X)$ denotes their joint probability density function (PDF), $B(X)$ is the line brightness defined in such a way that $I(\omega,X)$ is area-normalized. This quantity is usually obtained from a collisional-radiative model. As an example, we consider here the D_{10} line, in the presence of density fluctuations. The shape of this line is governed by the Stark effect and therefore is strongly dependent on the density. The brightness is roughly proportional to N^{α} with α close to unity. Figure 6 shows a plot of D_{10}, obtained assuming a Gamma PDF for the density fluctuations with $\langle N_e \rangle = 10^{13}$ cm^{-3} and $\Delta N_e/\langle N_e \rangle = 50\%$ (with ΔN_e being the root mean square). Such a large fluctuation rate has already been detected in edge plasmas [17]. The temperatures T_e, T_i have been set equal to 1 eV. As can be seen, the density fluctuations lead to a weak broadening of the line shape, by less than 20%. This result would suggest that passive spectroscopy diagnostics based on Stark broadening are robust, at least for moderate fluctuation rate. A much stronger deviation is expected in the case of electron temperature fluctuations, because the brightness has a strong, non-monotonic dependence on this parameter [8]. To illustrate it we consider a spectral line broadened due to the Doppler effect only, e.g. Dα at low-density conditions, and assume correlated fluctuations of T_e and T_{at}. We focus on one component of the Zeeman Lorentz triplet and we note $T_e = T_{\mathrm{at}} \equiv$ T. Figure 7 shows a profile of Dα with 50% of temperature fluctuations compared to the same profile without fluctuations, (a) for $\langle T \rangle = 20$ eV and (b) for $\langle T \rangle = 1$ eV, obtained with a Gamma PDF for the temperature. The brightness has been obtained from the collisional-radiative code SOPHIA [18]. The line width is strongly sensitive on the average temperature, in particular on its relative value with respect to the brightness' maximum value. The line shape is narrowed if $\langle T \rangle$ is significantly larger than the brightness maximum [case (a)]. This strong dependence on the average temperature is of interest for diagnostics. Note, the system considered here was ideal, with only one fluctuating parameter; a complementary work on the case where several parameters fluctuate at the same time should also be carried out.

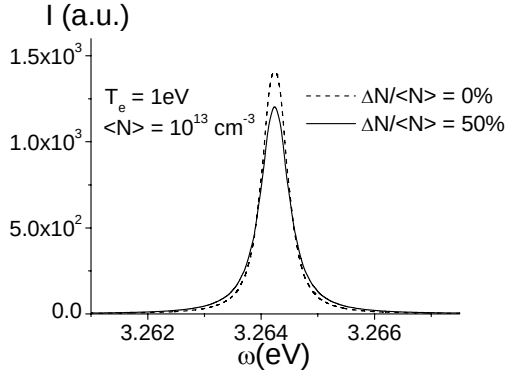

Figure 6. Profile of D_{10} with 50% of density fluctuations compared to the same profile without fluctuations, with $\langle N_e \rangle = 10^{13}$ cm^{-3} and $T_e = T_i = 1$ eV. In this particular case, the spectrum is scarcely affected by the fluctuations.

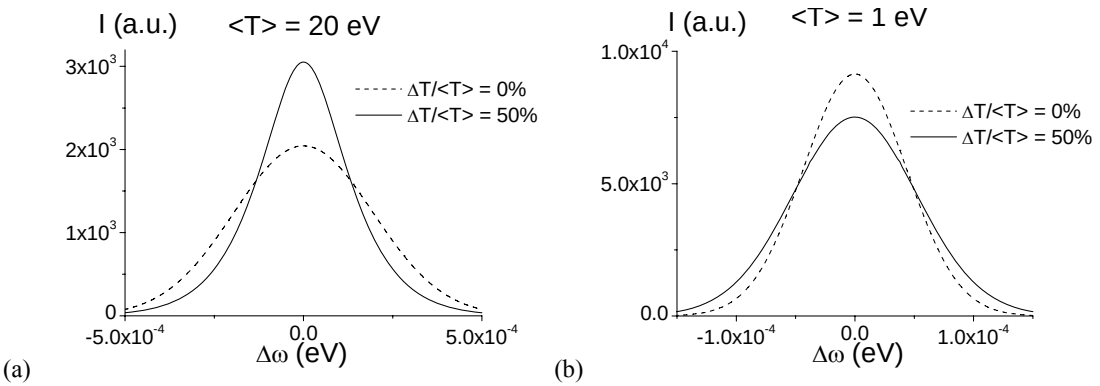

Figure 7. Profile of Dα with 50% of temperature fluctuations compared to the same profile without fluctuations, (a) for <T> = 20 eV and (b) for <T> = 1 eV. The width is strongly sensitive on the average temperature. In the case (a), the fluctuations lead to a narrowing of the profile.

6. Conclusion

The operation of ITER will require passive spectroscopy diagnostics in the edge plasma regions. In this work, we have assessed Balmer lines by using a line shape code and a plasma edge code. As a result, it is shown that low-*n* lines like Hα can be affected by Stark broadening significantly. In general, the Stark effect cannot be described by a simple analytical model. In spite of this, the use of a fitting routine with a three-Voigt function model could permit an extraction of the atomic temperature in a localized region with a quite good accuracy. In a similar way, it has been shown that local information on the electron density can also be obtained from analysis of the width of high-*n* lines. The role of turbulent fluctuations on line broadening has been examined through ideal cases. In particular, it has been shown that temperature fluctuations may lead to a significant modification of Doppler line shapes. The work presented in this paper provides additional information on what can be extracted from passive spectroscopy analysis in ITER. Further work could consist in similar investigations in pure helium discharges. The line radiation due to the impurities (viz. Be, C, W) should be also addressed, both regarding the shapes and the intensities, in equilibrium or in the presence of fluctuations (as done for lithium in [19,20]). Another issue of interest concerns the modeling of resonance lines, affected by opacity effects, in the presence of turbulence. Preliminary investigations have indicated a strong correlation between opaque lines and turbulence properties that could be used for diagnostics [21,22].

Acknowledgements

This work was carried out within the framework of the European Fusion Development Agreement and the French Research Federation for Fusion Studies. It is supported by the European Communities under the contract of Association between Euratom and CEA. The views and opinions expressed herein do not necessarily reflect those of the European Commission. Financial support was also received from the Agence Nationale de la Recherche, project ANR-11-BS09-023 (SEDIBA).

References

[1] Donné A J H *et al* 2007 *Nucl. Fusion* **47** S337–84
[2] Koubiti M, Loch S, Capes H, Godbert-Mouret L, Marandet Y, Meigs A, Stamm R and Summers H 2003 *J. Quant. Spectrosc. Radiat. Transfer* **81** 265–73
[3] Welch B L, Griem H R, Terry J, Kurz C, LaBombard B, Lipschultz B, Marmar E and McCracken G 1995 *Phys. Plasmas* **2** 4246–51
[4] Kotov V, Reiter D and Kukushkin A S 2007 *Forschungszentrum Jülich Report* Jül-4257
[5] Rosato J, Kotov V and Reiter D 2010 *J. Phys. B: At. Mol. Opt. Phys.* **43** 144024

[6] Rosato J, Kotov V, Reiter D, Capes H, Godbert-Mouret L, Koubiti M, Marandet Y and Stamm 2010 *AIP Conf. Proc.* **1290** 63–7
[7] Marandet Y, Capes H, Godbert-Mouret L, Koubiti M and Stamm R 2005 *Europhys. Lett.* **69** 531–7
[8] Rosato J, Capes H, Marandet Y, Rosmej F B, Stamm R, Godbert-Mouret L and Koubiti M 2008 *Europhys. Lett.* **84** 43002
[9] Marandet Y, Rosato J, Capes H, Godbert-Mouret L, Koubiti M, Mekkaoui A, Rosmej F B and Stamm R 2009 *High Energ. Dens. Phys.* **5** 312–9
[10] Griem H R 1974 *Spectral Line Broadening by Plasmas* (New York: Academic)
[11] Stamm R, Smith E W and Talin B 1984 *Phys. Rev. A* **30** 2039–46
[12] Gigosos M A, Fraile J and Torres F 1985 *Phys. Rev. A* **31** 3509–11
[13] Stambulchik E, Alexiou S, Griem H R and Kepple P C 2007 *Phys. Rev. E* **75** 016401
[14] Rosato J, Marandet Y, Capes H, Ferri S, Mossé C, Godbert-Mouret L, Koubiti M and Stamm R 2009 *Phys. Rev. E* **79** 046408
[15] Griem H R, Kolb A C and Shen K Y 1959 *Phys. Rev.* **116** 4–16
[16] Charbonneau P 1995 *Astrophys. J. Suppl. Ser.* **101** 309–34
[17] Boedo J A 2009 *J. Nucl. Mater.* **390–391** 29–37
[18] Rosmej F B, Stamm R, Fritzsche S, Capes H, Koubiti M, Marandet Y, Lisitsa V S, Ohno N, Takamura S and Nishijima D 2005 *J. Nucl. Mater.* **337–339** 1101–5
[19] Rosato J, Capes H, Catoire F, Kadomtsev M B, Levashova M G, Lisitsa V S, Marandet Y, Rosmej F B and Stamm R 2011 *J. Nucl. Mater.* **415** S617–9
[20] Rosato J, Catoire F, Marandet Y, Mekkaoui A, Capes H, Koubiti M, Stamm R, Kadomtsev M B, Levashova M G, Lisitsa V S and Rosmej F B 2011 *Phys. Lett. A* **375** 4187–9
[21] Rosato J, Reiter D, Marandet Y and Mekkaoui A 2009 *ECA* **33E** P5.155
[22] Rosato J, Mekkaoui A, Marandet Y, Reiter D, Kotov V, Capes H, Godbert-Mouret L, Koubiti M and Stamm R 2012 *Contrib. Plasma Phys.* **52** 429–34